Design of a Neural Network Controller for a Slung-Load System Lifted by 1 Quad-Rotor

Byung-Yoon Lee
Department of Aerospace Engineering, KAIST, Daejeon, Korea
Email: bylee@fdcl.kaist.ac.kr

Seong-Min Hong, Dong-Wan Yoo, Hae-In Lee, Gun-Hee Moon, and Min-Jea Tahk
Department of Aerospace Engineering, KAIST, Daejeon, Korea
Email: {smhong, dwyoo, hilee13, ghmoon, mjtahk}@fdcl.kaist.ac.kr

***Abstract*—This paper deals with the design of neural network controller for the slung-load system. There are many methods for modeling the slung-load system, we developed the entire system model based on the UKE (Udwadia-Kalaba Equations) in order to account for multi-constraints. Neural network was adapted to the attitude controller. Finally, considering all matters in the design process, numerical simulations are performed in order to verify the system model.**

***Index Terms*—slung-load system, Udwadia-Kalaba equation, quad-rotor, neural network, adaptive control**

I. Introduction

Recently, Unmanned Aerial Vehicles (UAVs) are used in many military purposes such as reconnaissance, observation or freight transportation. UAVs have a strong advantage regarding on pilot safety and cost reduction. Among them, quad-rotor has a capability of hovering and simple control logic, so many researchers have used quad-rotors as a platform of their own missions.

This research focuses on the design of neural network controller for slung-load system. For designing the controller of multi quad-rotors cooperative system, to design the controller of one quad-rotor system would be the first step. To derive the mathematical model of this system, we can find similar researches produced by Bisgaard *et al*., Sampath, Ronen *et al*., Cicolani *et al.* and Oh *et al.* [1]-[5]. Especially in this paper, we used the generic slung-load system model derived by Bisgaard *et al*. which is based on Udwadia-Kalaba Equation (UKE), that analyze the existing modeling method and consider the constraints proposed by Udwadia *et al.* [1], [6].

In order to obtain improved performance and eliminate the requirements for gain scheduling, model inversion method based on feedback linearization has been introduced. Dynamic model inversion generates error which is produced by contradiction with nonlinear model. Thus, we adapt another notion of on-line adaptive neural network. The deficient information of modeling can be supplied by on-line learning process of Sigma-Pi neural network [8].

In this paper, using these techniques; UKE, feedback linearization and adaptive neural networks, an analysis of position and attitude control performance is simulated.

An organization of this paper is described as follows. First, the Udwadia-Kalaba modeling principle is introduced in chapter 2. Then, the quad-rotor modeling process with position and attitude controller is presented in chapter 3. In chapter 4, methodology regarding on adaptive neural network is described. The simulation results are included in chapter 5. Finally, there are conclusion and further research plans in chapter 6.

II. Modeling of the Slung-Load System

A new aspect on the system including constrained condition generated the new principle of dynamic system modeling. The UKE is based on Gauss' principle of least constraint and yields an explicit equation. The result of this equation and principles of Lagrange are equivalent [7]. More specific derivation process can be seen [6].

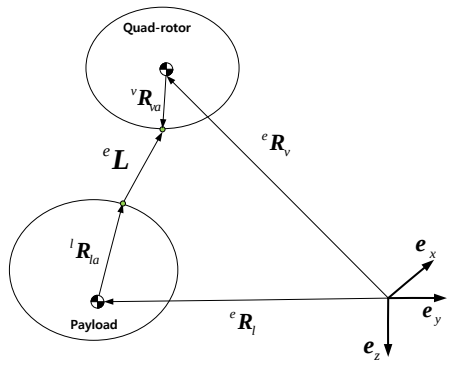

Figure 1. Slung-load system modeling

Fig. 1 describes the overall model of the system. The rigid body modeling is derived with respect to the inertial frame denoted as the NED frame, oriented with the z axis pointing the center of the Earth, x axis pointing north and y axis pointing east with notation ${}^{e}(\cdot)$. Body-fixed frame coordinate systems are defined at the center of mass for the quad-rotor and payload. The notation

Manuscript received October 15, 2013; received February 10, 2014.

doi: 10.12720/joace.3.1.9-14

${}^{v}(\cdot)$ is for the quad-rotor vehicle, ${}^{l}(\cdot)$ is for the load. The additional subscript a denotes the 'attaching point' of the wire and each object.

The wire vector ${}^{e}L$ can be expressed as the following equation.

$$ {}^{e}L = {}^{e}R_v + C_{ev}\,{}^{v}R_{va} - {}^{e}R_l - C_{el}\,{}^{l}R_{la} \tag{1} $$

In (1), the transformation matrix C_{ev} represents the direction cosine matrix (DCM) that maps from the body of quad-rotor to the Earth frame, also the transformation matrix C_{el} maps from l coordinate to the Earth. The wire vector is a function of the position vectors of the quad-rotor ${}^{e}R_v$ and the load ${}^{e}R_l$ also the position vectors pointing attaching point on the quad-rotor ${}^{v}R_{va}$ and the load ${}^{l}R_{la}$. Then, it needs to be differentiated twice to obtain the generic form of constraint equation in [6]. The constraint equation is given by

$$ g(q) = \left\| {}^{e}L \right\|^2 - l^2 = \left({}^{e}L \right)^T \left({}^{e}L \right) - l^2 \tag{2} $$

where l is the nominal undeformed length of the wire. As mentioned above, the (2) is differentiated twice and this yields

$$ \dot{g}(q) = 0 = 2\,{}^{e}\dot{L}^{T}\,{}^{e}L \tag{3} $$

$$ \ddot{g}(q) = 0 = 2\,{}^{e}\ddot{L}^{T}\,{}^{e}L + 2\,{}^{e}\dot{L}^{T}\,{}^{e}\dot{L} \tag{4} $$

In (3) and (4), ${}^{e}\dot{L}$ and ${}^{e}\ddot{L}$ can be easily obtain by differentiating the (1).

$$ {}^{e}\dot{L} = {}^{e}\dot{R}_v - {}^{e}\dot{R}_l + \dot{C}_{ev}\,{}^{v}R_{va} - \dot{C}_{el}\,{}^{l}R_{la} \tag{5} $$

$$ {}^{e}\ddot{L} = {}^{e}\ddot{R}_v - {}^{e}\ddot{R}_l + \ddot{C}_{ev}\,{}^{v}R_{va} - \ddot{C}_{el}\,{}^{l}R_{la} \tag{6} $$

Now, first and second order derivative of DCMs in (5) and (6) can be transformed by using relationship in [1]. Substituting the result of it into (5) and (6) yields

$$ {}^{e}\dot{L} = C_{ev}\,{}^{v}v_v - C_{el}\,{}^{l}v_l + C_{ev}\,{}^{v}\tilde{\omega}_v R_{va} - C_{el}\,{}^{l}\tilde{\omega}_l R_{la} \tag{7} $$

$$ \begin{aligned} {}^{e}\ddot{L} = {} & C_{ev}\,{}^{v}a_v - C_{el}\,{}^{l}a_l + C_{ev}\,{}^{v}\dot{\tilde{\omega}}_v R_{va} - C_{el}\,{}^{l}\dot{\tilde{\omega}}_l R_{la} \\ & + C_{ev}\,{}^{v}\tilde{\omega}_v\,{}^{v}\tilde{\omega}_v R_{va} - C_{el}\,{}^{l}\tilde{\omega}_l\,{}^{l}\tilde{\omega}_l R_{la} \end{aligned} \tag{8} $$

Then, to obtain final constraint equation, (7) and (8) are substitute into (4) and this yields

$$ \ddot{g}(q) = 2\,{}^{e}L^{T}(C_{ev}\,{}^{v}a_v - C_{el}\,{}^{l}a_l - C_{ev}\tilde{R}_{va}\,{}^{v}\alpha_v + C_{el}\tilde{R}_{la}\,{}^{l}\alpha_l) - b \tag{9} $$

where b is the acceleration independent term as

$$ \begin{aligned} b = {} & -2\,{}^{e}\dot{L}^{T\,e}\dot{L} - 2\,{}^{e}L^{T}(C_{ev}\,{}^{v}\tilde{\omega}_v\,{}^{v}\tilde{\omega}_v R_{va} - C_{el}\,{}^{l}\tilde{\omega}_l\,{}^{l}\tilde{\omega}_l R_{la} \\ & + C_{ev}\tilde{R}_{va} I_v^{-1\,v}\tilde{\omega}_v I_v\,{}^{v}\omega_v - C_{el}\tilde{R}_{la} I_l^{-1\,l}\tilde{\omega}_l I_l\,{}^{l}\omega_l) \end{aligned} \tag{10} $$

Finally, matrix A is identified as

$$ A = 2\,{}^{e}L^{T}\begin{bmatrix} C_{ev} & -C_{ev}\tilde{R}_{va} & -C_{el} & C_{el}\tilde{R}_{la} \end{bmatrix} \tag{11} $$

III. Quad-Rotor Modeling

A. Quad-Rotor Dynamics

Fig. 2 shows typical quad-rotor structure. This quad-rotor structure includes four rotors which are mounted on the tip of cross-shaped rods.

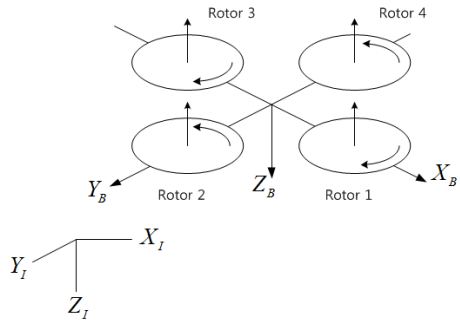

Figure 2. Quad-rotor configuration

Four rotors are defined as rotor number 1, 2, 3, and 4 in clockwise direction from the front of the quad-rotor. Euler angles of quad-rotor are changed by applying the angular velocity differences on these four rotors. We define the angular velocities of four rotors as Ω_1, Ω_2, Ω_3, and Ω_4, and these actuator system is modeled as the first order system. Mathematical model of actuator system is represents in (12). K_t is the motor thrust coefficient and K_r is the motor torque coefficient. Therefore, force T and torque τ_r can be determined by (12). There are four rotors on the quad-rotor, so forces acting in each direction of the quad-rotor are expressed in (13). The moments acting on each angular direction of the quad-rotor are shown in (14), and these equations are including gyroscopic effect.

$$ \begin{aligned} T &= K_t \Omega_i^{\,2} \\ \tau_r &= K_r \Omega_i^{\,2} \end{aligned} \tag{12} $$

$$ \begin{aligned} F_x &= F_y = 0 \\ F_z &= -K_t(\Omega_1^{\,2} + \Omega_2^{\,2} + \Omega_3^{\,2} + \Omega_4^{\,2}) \end{aligned} \tag{13} $$

$$ \begin{aligned} L &= K_t(-\Omega_2^{\,2} + \Omega_4^{\,2})d - I_r q(\Omega_1 - \Omega_2 + \Omega_3 - \Omega_4) \\ M &= K_t(\Omega_1^{\,2} + \Omega_3^{\,2})d + I_r p(\Omega_1 - \Omega_2 + \Omega_3 - \Omega_4) \\ N &= K_r(-\Omega_1^{\,2} + \Omega_2^{\,2} - \Omega_3^{\,2} + \Omega_4^{\,2}) \end{aligned} \tag{14} $$

B. Quad-Rotor Control Allocation

In this paper, we determine control commands as δ_ϕ, δ_θ, and δ_ψ. In more detail, these control commands are the rotor angular velocity differences that generate each-axis torque of the quad-rotor. Likewise, δ_z is the rotor angular velocity difference that generates vertical direction force of the quad-rotor. Equation (15) represents the control allocation logic of the quad-rotor.

$$ \begin{aligned} \Omega_1 &= \Omega_{nom} + (\delta_z/4) + (\delta_\theta/2) - (\delta_\psi/4) \\ \Omega_2 &= \Omega_{nom} + (\delta_z/4) - (\delta_\phi/2) + (\delta_\psi/4) \\ \Omega_3 &= \Omega_{nom} + (\delta_z/4) - (\delta_\theta/2) - (\delta_\psi/4) \\ \Omega_4 &= \Omega_{nom} + (\delta_z/4) + (\delta_\phi/2) + (\delta_\psi/4) \end{aligned} \tag{15} $$

C. Attitude Control

Attitude control is for the tracking and maintaining Euler angles of the quad-rotor. In this paper, conventional PD attitude control method is using to implement adaptive neural network attitude controller. First of all, we use PD control method for designing attitude controller. Equations and structure of PD attitude controller are shown in (16) and Fig. 3.

$$\begin{aligned}\delta_\phi &= K_{d,\phi}(K_{p,\phi}(\phi_{cmd}-\phi)-p)\\ \delta_\theta &= K_{d,\theta}(K_{p,\theta}(\theta_{cmd}-\theta)-q)\\ \delta_\psi &= K_{d,\psi}(K_{p,\psi}(\psi_{cmd}-\psi)-r)\end{aligned} \tag{16}$$

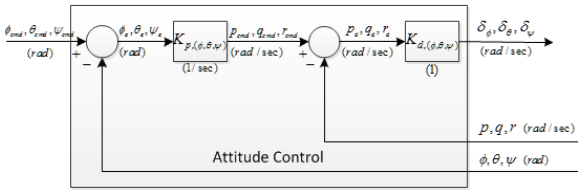

Figure 3. PD attitude controller

D. Position Control

Goal of the position control is to locate the quad-rotor at the desired position in the inertial frame. For this purpose, the position controller contains the attitude controller as an inner loop structure as shown in Fig. 3. Therefore, Euler angle commands ϕ_{cmd} and θ_{cmd} should be the output of the position controller. In addition, these two commands are changed by difference of yaw angle ψ.

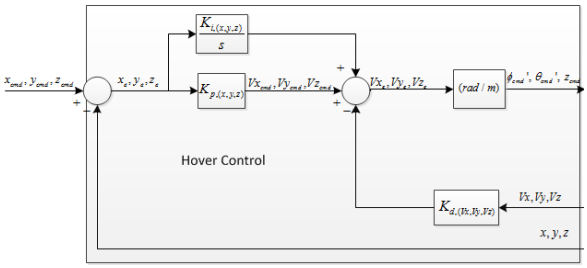

Figure 4. PID position controller

We use conventional PID control method and the output of the position controller are denoted as θ_{cmd}' and ϕ_{cmd}'. By using these outputs with nonzero yaw angle ψ, we can calculate Euler angle commands ϕ_{cmd} and θ_{cmd} with respect to the body frame. Equations of the position controller are expressed in (17), (18), and (19). Structure of the position controller is shown in Fig. 4.

$$\begin{aligned}\phi_{cmd} &= -[(K_{p,x}(x_{cmd}-x)-K_{d,x}Vx)+\frac{K_{i,x}}{s}]\sin\psi\\ &\quad +[(K_{p,y}(y_{cmd}-y)-K_{d,y}Vy)+\frac{K_{i,y}}{s}]\cos\psi\\ &= -\theta_{cmd}'\sin\psi+\phi_{cmd}'\cos\psi\end{aligned} \tag{17}$$

$$\begin{aligned}\theta_{cmd} &= -[(K_{p,x}(x_{cmd}-x)-K_{d,x}Vx)+\frac{K_{i,x}}{s}]\cos\psi\\ &\quad -[(K_{p,y}(y_{cmd}-y)-K_{d,y}Vy)+\frac{K_{i,y}}{s}]\sin\psi\\ &= -\theta_{cmd}'\cos\psi-\phi_{cmd}'\sin\psi\end{aligned} \tag{18}$$

$$\Delta\Omega_z = -(K_{p,z}(z_{cmd}-z)-K_{d,z}Vz)+\frac{K_{i,z}}{s} \tag{19}$$

IV. Adaptive Neural Networks

A. Adaptive Control Structure

In this paper, we use feedback linearization method to use on-line adaptive neural networks [9]. According to feedback linearization method, adaptive controller is required to eliminate the inversion error Δ'. This adaptive control structure is given in Fig. 5. Adaptive control signal $\hat{u}_{ad}$ is generated by on-line neural network to support the PD control signal.

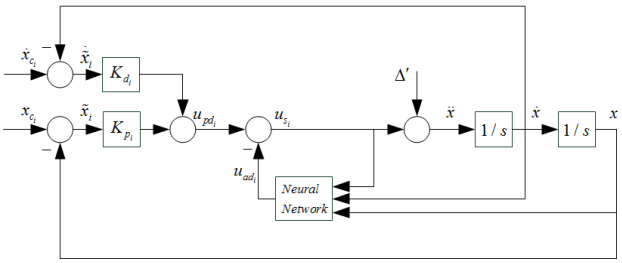

Figure 5. Adaptive control structure

B. Approximate Model Inversion

Nonlinear dynamics of the quad-rotor is approximated to linear system to model inversion technique is applicable [10]. The quad-rotor dynamics inversion consists of two parts, which are implemented in attitude and position controller respectively.

First of all, dynamics from pitch and roll attributes to longitudinal and lateral accelerations is inverted in order to obtain required pitch and roll angles ($\bar{\theta}$, $\bar{\phi}$) from pseudo-commands (u_x, u_y, u_z) and yaw command (ψ_c). Considering that forces along x- and y-axis are ignorant compared to force along z-axis, the inverted model can be presented as (20) and (21). With these equations, F_z can be derived from (22).

$$\bar{\theta} = \arctan\left(\frac{u_x\cos\psi_c + u_y\sin\psi_c}{u_z - g}\right) \tag{20}$$

$$\bar{\phi} = \arctan\left(\frac{u_x\sin\psi_c - u_y\cos\psi_c}{F_z/m}\right) \tag{21}$$

$$\left(\frac{F_z}{m}\right)^2 = u_x^2 + u_y^2 + (u_z - g)^2 \tag{22}$$

Secondly, dynamics from collective commands to attitude changes is inverted. Substituting the relationship between pseudo-commands (u_ϕ , u_θ , u_ψ) and the quad-rotor attitude change, amount of varying collective commands ($\Delta\delta_a$, $\Delta\delta_e$, $\Delta\delta_p$, $\Delta\delta_c$) can be derived as (23) and (24) in [11]. Finally, the quad-rotor attitude commands are given as (25).

$$\begin{bmatrix} \Delta\delta_a \\ \Delta\delta_e \\ \Delta\delta_p \end{bmatrix} = B^{-1}\left(\begin{bmatrix} \dot{p}_c & \dot{q}_c & \dot{r}_c \end{bmatrix}^T - A\begin{bmatrix} p & q & r & u & v & w \end{bmatrix}^T\right) \quad (23)$$

$$\Delta\delta_c = \left(\frac{F_z}{m} - g\right) \Big/ Z_{\delta_c} \quad (24)$$

$$\begin{aligned} \dot{p}_C &= u_\phi - u_\psi \sin\theta - \dot{\psi}\dot{\theta}\cos\theta \\ \dot{q}_C &= u_\theta \cos\phi - \dot{\theta}\dot{\phi}\sin\phi + u_\psi \sin\phi\cos\theta + \dot{\psi}\dot{\phi}\cos\phi\cos\theta - \dot{\psi}\dot{\phi}\sin\phi\sin\theta \\ \dot{r}_C &= -u_\theta \sin\phi - \dot{\theta}\dot{\phi}\cos\phi + u_\psi \cos\phi\cos\theta + \dot{\psi}\dot{\phi}\sin\phi\cos\theta - \dot{\psi}\dot{\phi}\cos\phi\sin\theta \end{aligned} \quad (25)$$

V. Simulation

A. Simulation Setup

In this paper, properties of the quad-rotor are determined using [12]. In addition, we assumed that properties of the payload are equal to Table I. Therefore parameters of the quad-rotor and payload are shown in Table I.

TABLE I. Parameters of the Quad-Rotor and Payload

Description	Value	Description	Value	Unit
Quad-rotor Mass	50.0	Payload Mass	5.0	kg
Quad-rotor MOI (X-axis)	10.0	Payload MOI (X-axis)	1.0	$kg \cdot m^2$
Quad-rotor MOI (Y-axis)	10.0	Payload MOI (Y-axis)	1.0	$kg \cdot m^2$
Quad-rotor MOI (Z-axis)	10.0	Payload MOI (Z-axis)	1.0	$kg \cdot m^2$
Quad-rotor rotor inertia	5.142×10^{-2}	-	-	$kg \cdot m^2$
Distance (motor to c.g)	2.0	-	-	m

Using these parameters of the quad-rotor and payload, we performed 1-vehicle 1-payload slung-load position control simulation to show attitude and position tracking performance of the adaptive neural network. Table II shows that waypoint sequence of position control simulation.

TABLE II. Waypoint Sequence

Waypoint	N (m)	E (m)	D (m)	Psi angle (deg)
0	0	0	-4	0
1	0	8	-4	0
2	8	8	-4	0
3	8	0	-8	0
4	0	0	-8	0
5	0	0	-4	0

B. Simulation Results

Using the previous simulation setup, result graphs are shown below. Fig. 6 represents simulation results of the quad-rotor position and attitude. As can be observed from Fig. 6, position and attitude of the quad-rotor are successfully trace reference command signal. Especially, attitude controller shows impressive performance through the efforts of adaptive neural network.

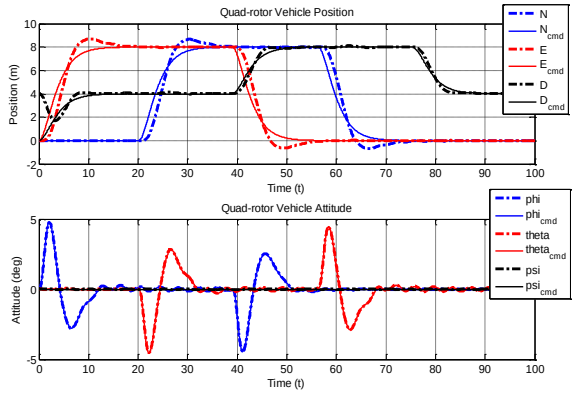

Figure 6. Simulation results of the quad-rotor position and attitude

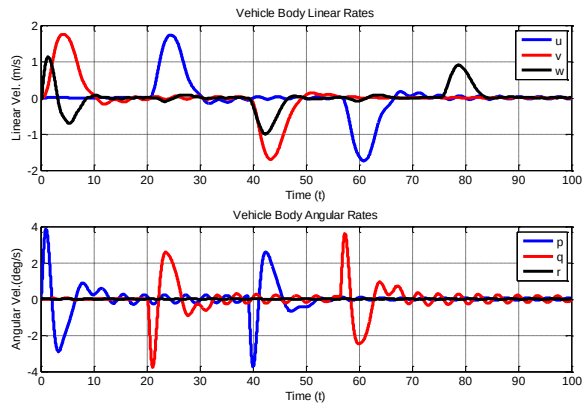

Figure 7. Simulation results of the quad-rotor linear rates and angular rates

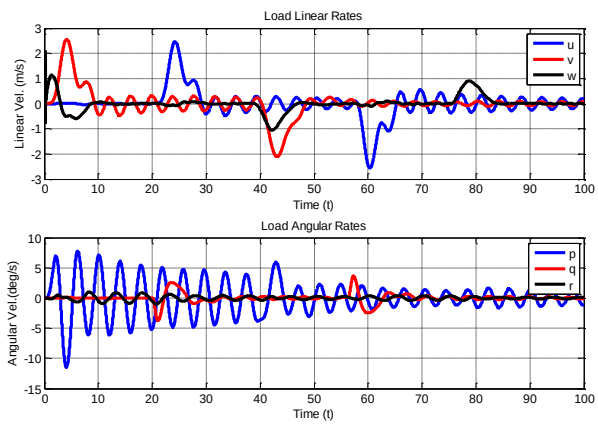

Figure 8. Simulation results of the payload position and attitude

Fig. 7 shows simulations results of the quad-rotor linear rates and angular rates. Simulation results of the payload position and attitude are shown in Fig. 8. From the observed results of these graphs, we know that

position and attitude of the quad-rotor did not diverge despite of oscillating motion of the payload. Also, simulation results of the payload linear rates and angular rates are shown in Fig. 9.

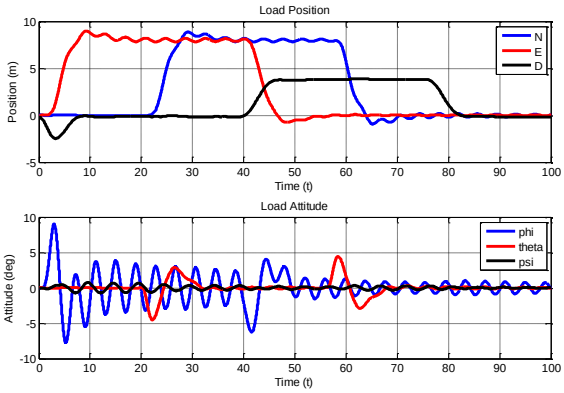

Figure 9. Simulation results of the payload linear rates and angular rates

As a result, we can obtain 3D-Plot of simulation results as Fig. 10.

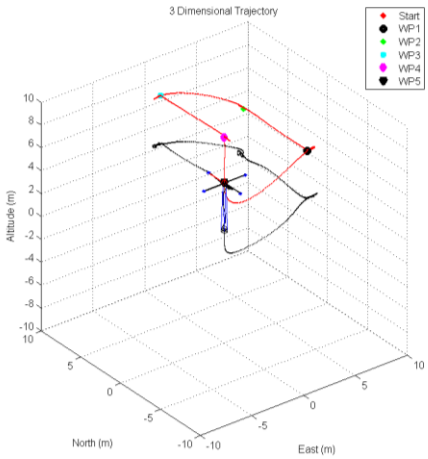

Figure 10. 3D-Plot of simulation results

VI. Conclusion

In this paper, slung-load dynamics are used to perform simulation environment of the transportation of 1 quad-rotor with 1 payload. To control this quad-rotor, we used adaptive neural network for the quad-rotor attitude control. This adaptive neural network is used to control 1 quad-rotor with 1 payload. In fact, this neural network controller is designed for only 1 quad-rotor without any payload. However, from simulation results, we show that this neural network controller works well with 1 quad-rotor with 1 payload also. For further research, approximate model inversion method will be re-derived with slung-load dynamics. In addition, performance of designed adaptive neural network controller will be tested by real flight test.

Acknowledgment

This research was supported by Defense Acquisition Program Administration and Agency for Defense Development under the contract UE124026JD.

References

[1] M. Bisgaard, J. Bendtsen, and A. Cour-Harbo, "Modeling of generic slung load system," *Journal of Guidance, Control, and Dynamics*, vol. 32, no. 2, pp. 573-585, August 2006.

[2] P. Sampath, "Dynamics of a helicopter-slung load system," MD, Univ. of Maryland, 1980.

[3] T. Ronen, A. E. Bryson, and W. S. Hindson, "Dynamics of a helicopter with a sling load," presented at the AIAA Atmospheric Flight Mechanics Conference, 1986.

[4] L. S. Cicolani and G. Kanning, *Equations of Motion of Slung-Load Systems, Including Multilift Systems*, NASA, 1992.

[5] H. Oh, M. Tahk, and Y. Kim, "Modeling of a slung load system lifted by 2 quad-rotors (QRVs)," presented at the KSAS Spring Conference, Jeongsun, Korea, 2013.

[6] F. Udwadia and R. Kalaba, "Equations of motion for mechanical systems," *Journal of Aerospace Engineering*, vol. 9, no. 3, pp. 64-69, 1996.

[7] L. B. Lucassen and F. J. Sterk, "Dynamic stability analysis of a hovering helicopter with a sling load," *Journal of the American Helicopter Society*, vol. 10, pp. 6-12, April 1965.

[8] B. S. Kim and A. J. Calise, "Nonlinear flight control using neural networks," *Journal of Guidance, Control, and Dynamics*, vol. 20, no. 1, pp. 26-33, 1997.

[9] J. V. R. Prasad and A. M. Lipp, "Synthesis of a helicopter nonlinear flight controller using approximate model inversion," *Mathematical and Computer Modelling*, vol. 18, no. 3/4, pp. 89-100, 1993.

[10] J. Leitner, A. J. Calise, and J. V. R. Prasad, "Analysis of adaptive neural networks for helicopter flight control," *Journal of Guidance, Control, and Dynamics*, vol. 20, no. 5, pp. 972-979, 1997.

[11] J. V. R. Prasad, A. J. Calise, and Y. Pei, "Adaptive nonlinear controller synthesis and flight test evaluation on an unmanned helicopter," presented at the IEEE International Conference on Control Applications, 1999.

[12] B. Y. Lee, D. W. Yoo, and M. J. Tahk, "Attitude control system design for aggressive maneuver of a quad-rotor UAV," presented at the 32nd IASTED International Conference, February 11-13, 2013.

Byung-Yoon Lee was born in the Seoul, Korea in 1984 and received B.S. degree in electronic and computer engineering from Kyunghee University, Gyonggi-do, Korea, in 2010. He is presently a Ph.D. Student of Aerospace Engineering at Korea Advanced Institute of Science and Technology, Daejeon, Korea. His research interests include flight control system design and cooperative control system design of multiple UAVs.

Seong-Min Hong was born in the Daegu, Korea in 1988 and received B.S. degree in mechanical engineering from Sungkyunkwan University, Suwon, Korea, in 2013. He is presently a Master's Student of Aerospace Engineering at Korea Advanced Institute of Science and Technology, Daejeon, Korea. His research interests include flight control design and missile guidance.

Dong-Wan Yoo was born in the Seoul, Korea in 1984 and received B.S. degree from Pennsylvania State University, University Park PA, USA and the M.S. degree from Korea Advanced Institute of Science and Technology, Daejeon, Korea, all in aerospace engineering. He is currently a Ph.D. Student of Aerospace Engineering at Korea Advanced Institute of Science and Technology, Daejeon, Korea. His research interests include flight dynamics and control.

Hae-In Lee was born in Busan, Korea in 1991 and received B.S degree in aerospace engineering from Korea Advanced Institute of Science and Technology, Daejeon, Korea, in 2013. She is presently a Master's Student of aerospace engineering at Korea Advanced Institute of Science and Technology, Daejeon, Korea. Her research interests include flight control design and missile guidance.

Gun Hee Moon was born in Seoul, Korea, in 1990. He received the B.S. degree in aerospace engineering from the Inha University, Incheon, Korea, in 2012. He is currently pursuing the M.S. degree in aerospace engineering at Korea Advanced Institute of Science and Technology, Daejeon, Korea. His current research interests include decision making of multi agents over cooperative tasks and guidance and control of unmanned system.

Min-Jea Tahk was born in South Korea in 1954 and received the Ph.D. degrees in aerospace engineering from the University of Texas at Austin in 1986. He is currently a Professor of the department of aerospace engineering, Korea Advanced Institute of Science and Technology, Daejeon, Korea. His research areas include flight control, parameter optimization, modeling and simulation.